Chapter 5

Relaxation of a field-unwound cholesteric liquid crystal

5.1 Unwinding of a cholesteric liquid crystal

A cholesteric liquid crystal (ChLC) possesses a periodic helical structure due to the chirality of molecules. In a ChLC with a positive dielectric anisotropy ($\Delta\varepsilon > 0$), a field-induced cholesteric-nematic phase transition was theoretically predicted [1] and experimentally observed [2]. When the electric field is applied perpendicular to the helical axis of a ChLC with a planar texture, a stepwise change in the pitch with an increase in the field is theoretically predicted [3] and experimentally observed [4]. At sufficiently strong field strength, the field-induced homogeneous texture is obtained [1,5], as shown in Fig. 5.1. The critical field is given by $Ec = (\pi^2 / P_0) \times (K_{22} / \varepsilon_0 \Delta\varepsilon)^{1/2}$, where P_0 is the natural pitch of the ChLC and K_{22} is the twist elastic constant [1].

On the other hand, when the electric field is applied parallel to the helical axis, the ChLC layers may undergo sinusoidal periodic modulation under the application of a weak electric field. The modulation results from the frustration caused by the competition between the chirality, which favors a twist deformation, and the electric field, which favors alignment of molecules parallel to the field. The threshold field and period of the sinusoidal periodic deformation were first theoretically described

by Helfrich [6] and refined by Hurault [7] and Chigrinov [8], respectively. Kamien and Selinger theoretically predicted the structure of the sinusoidal deformation in which the chirality favors to form [9]. On increasing the electric field, a 90° rotation of the helical axis occurs and the fingerprint (or focal conic) texture forms. After the fingerprint texture is formed, the untwisting process of the helix with the increase of the electric field is similar to the cholesteric-homogeneous transition and the field-induced homeotropic texture is obtained [5], as shown in Fig. 5.1.
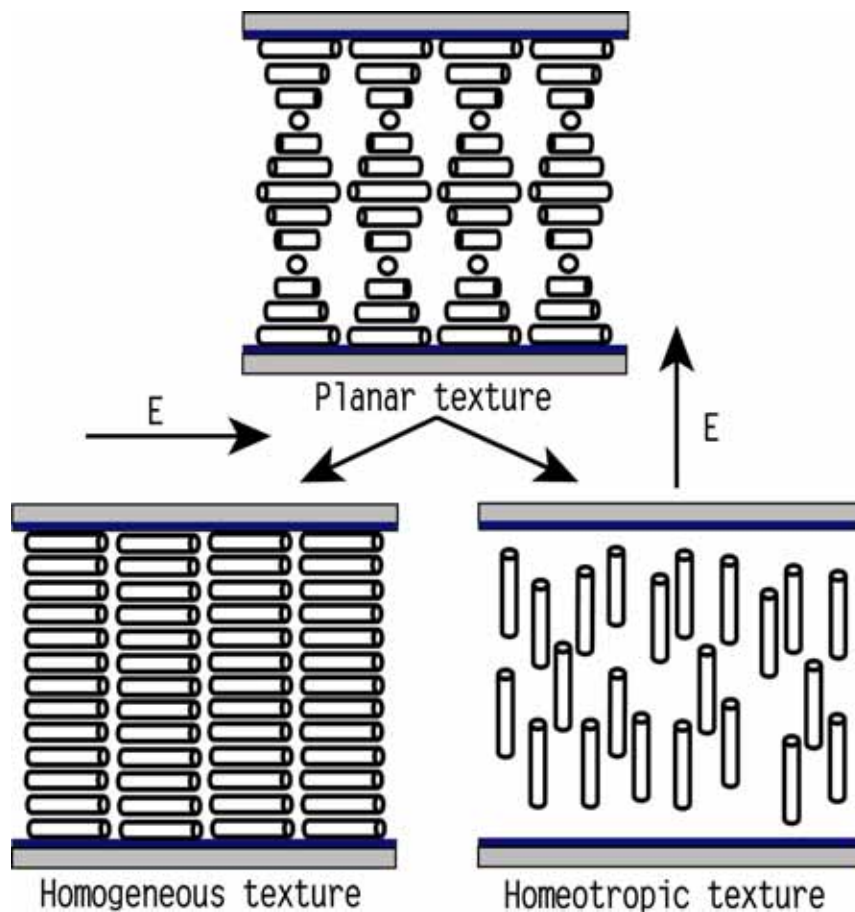

Figure 5.1 Schematic diagram of a field-unwound cholesteric liquid crystal. If the electric field is applied perpendicular to the helical axis, the field-induced homogeneous texture is obtained. If the electric field is applied parallel to the helical axis, the field-induced homeotropic texture is obtained.

When the external field is turned off abruptly, the relaxation process from the field-induced homogeneous or homeotropic texture to stable planar texture is frustrated and then will be accompanied by the Helfrich-like periodic modulation. This modulation is due to the frustration caused by the competition of chirality, which favors a twist deformation, and boundary constraints, which favor alignment of molecules parallel to the surfaces. Similar Helfrich-like periodic deformations have been observed in a planar-aligned ChLC by mechanically untwisting of the helix or by a temperature-induced pitch variation [10]. One can classify these Helfrich-like deformations into two types according to the driving sources for the deformation [11,12]. One is the field-induced Helfrich deformation. The other is the elastic-induced Helfrich deformation. In the former case, the ChLC layers undergo the sinusoidal deformation to alleviate the dielectric free energy of the system. However, for the latter case, the ChLC layers form the sinusoidal deformation in order to reduce the elastic free energy of the system.

In this chapter, we will numerically investigate the dynamic relaxation process from the field-induced homogeneous and homeotropic textures, respectively, to stable planar texture and show the transformation between textures. The transformation is an elastic-induced Helfrich deformation. We find that the relaxation process of a field-unwound ChLC occurs via an elastic-induced Helfrich deformation without introduction of defect cores.

5.2 Simulation method

For our modeling of the ChLC system, we exploit a similar simulation method to that discussed in section 3.2. In this simulation, we use periodic boundary conditions in the x and y directions. Dirichlet boundary conditions are assumed for the planes $Z = 0$ and $Z = d$ corresponding to strong anchoring. If the applied electric field is larger than Ec, the director at each node in the bulk can be initially assumed to be (1,0,0) and (0,0,1) for the field-induced homogeneous and homeotropic textures, respectively. When the electric field is turned off abruptly, some random noise is superposed on the initial bulk director configuration to avoid the system to be in the metasbable state. In the filed-induced homogeneous texture, we set n_y and n_z to random numbers between 0.1 and -0.1 then n_x can be determined based on the relationship $n_x=(1-n_y^2-n_z^2)^{1/2}$. On the other hand, in the filed-induced homeotropic texture, we set n_x and n_y to random numbers between 0.1 and -0.1 then n_z can be determined based on the relationship $n_z=(1-n_x^2-n_y^2)^{1/2}$. This random noise can be thought to be thermal fluctuations and it affects the director configuration very little.

In this simulation, the following LC parameters (Merk ZLI-4792) are used : $K_{11} = 13.2$ pN, $K_{22} = 6.5$ pN, $K_{33} = 18.3$ pN, $\Delta\varepsilon = 5.2$, $\varepsilon = 3.1$, and $\gamma_1 = 0.133$ Pas. The 3 % chiral agent (Merck S811) is doped into the above host, resulting in a natural pitch $P_0 = 2.98$ μm. The physical size of the cell in the calculation is assumed to be 6.4 μm and 6.4 μm in the X direction (rubbing direction) and Z direction (cell-normal direction), respectively, with 65×65 node points. Thus the thickness-to-pitch ratio (d/P_0) is 2.15. Fixed planar-aligned boundary conditions with a 4.0° pretilt angle are assumed.

5.3 Elastic-induced Helfrich deformation

In this section, we present our simulation results in the following manner. In part A, we present the relaxation process from the field-induced homogeneous texture to stable planar texture. In part B, we present the relaxation process from the field-induced homeotropic texture to stable planar texture. In each part, we will show the two-dimensional (X-Z plane) director configurations during the relaxation process of a field-unwound cholesteric liquid crystal. In these figures, the director at each node of the element is represented as a cylindrical. The orientation of the cylindrical indicates the average orientation of cholesteric liquid crystal molecules at the point in space associated with that node. For a clear view, these figures are drawn-sampled.

A. Homogeneous-planar relaxation

The planar-aligned cholesteric liquid crystal can be unwound to a homogeneous texture, as shown in Fig. 5.2(a), under the electric field is applied perpendicular to the helical axis and the field strength is larger than Ec. We will define time t = 0 as the time at which the voltage is removed. Due to the chiral parameter is not equal to zero, i.e., $q_0 \neq 0$, the cholesteric liquid crystal molecules incline to twist to planar texture. However, the boundary constraints hinder the twist deformation. Under the competition of chirality and boundary constraints, the molecules are seen to form the sinusoidal Helfrich deformation to alleviate the stored high twist energy, as shown in Fig. 5.2(b). This modulated structure matches the theoretical prediction [9]. Moreover, the wavelength of the Helfrich deformation roughly equals to the theoretical value derived by Chigrinov et al., which is induced by the external field [8]. The period is given as

$$\lambda = [P_0 d(3K_{33}/2K_{22})^{1/2}]^{1/2},$$ (1)

where d is the cell gap. Considering the parameters used in the simulation, one gets λ = 6.26 μm. As expected, there is one full wavelength in the X direction, as shown in Fig 5.2(b). Furthermore, the direction of Helfrich deformation is parallel to the director orientation at middle layer of the cell. Therefore, one will observe the striped direction perpendicular to the rubbing direction and this result agrees well with the previous experimental observation [4]. As can be seen in Fig 5.2(c), the amplitude of modulation increase with time and the twist deformation in the bulk occurs. Here, the modulation no longer exhibits a sinusoidal appearance, but rather appears to exhibit "fingers" that grow from the surfaces in a spatially alternating fashion. As time progresses, the ends of fingers spread out horizontally and overlap each other, as shown in Fig. 5.2(d). In this stage, cholesteric liquid crystals possess a nonequilibrium pitch length, hence, the layers proceed to distort and overlap each other to increase the number of pitches, as shown in Fig. 5.2(e). This results in the formation of the equilibrium region with intrinsic pitch and domain wall that separate the stable planar texture, as shown in Fig. 5.2(f). As expected, the equilibrium region has two full 360° twists ($d/P_0 = 2.15$).

The model obtained agrees well with previous experimental observation that for an abrupt turn-off of the relaxation of a field-unwound cholesteric liquid crystal is accompanied by the appearance of spatially modulated texture and this texture will then gradually convert into a stable planar texture with domain wall [4,14].
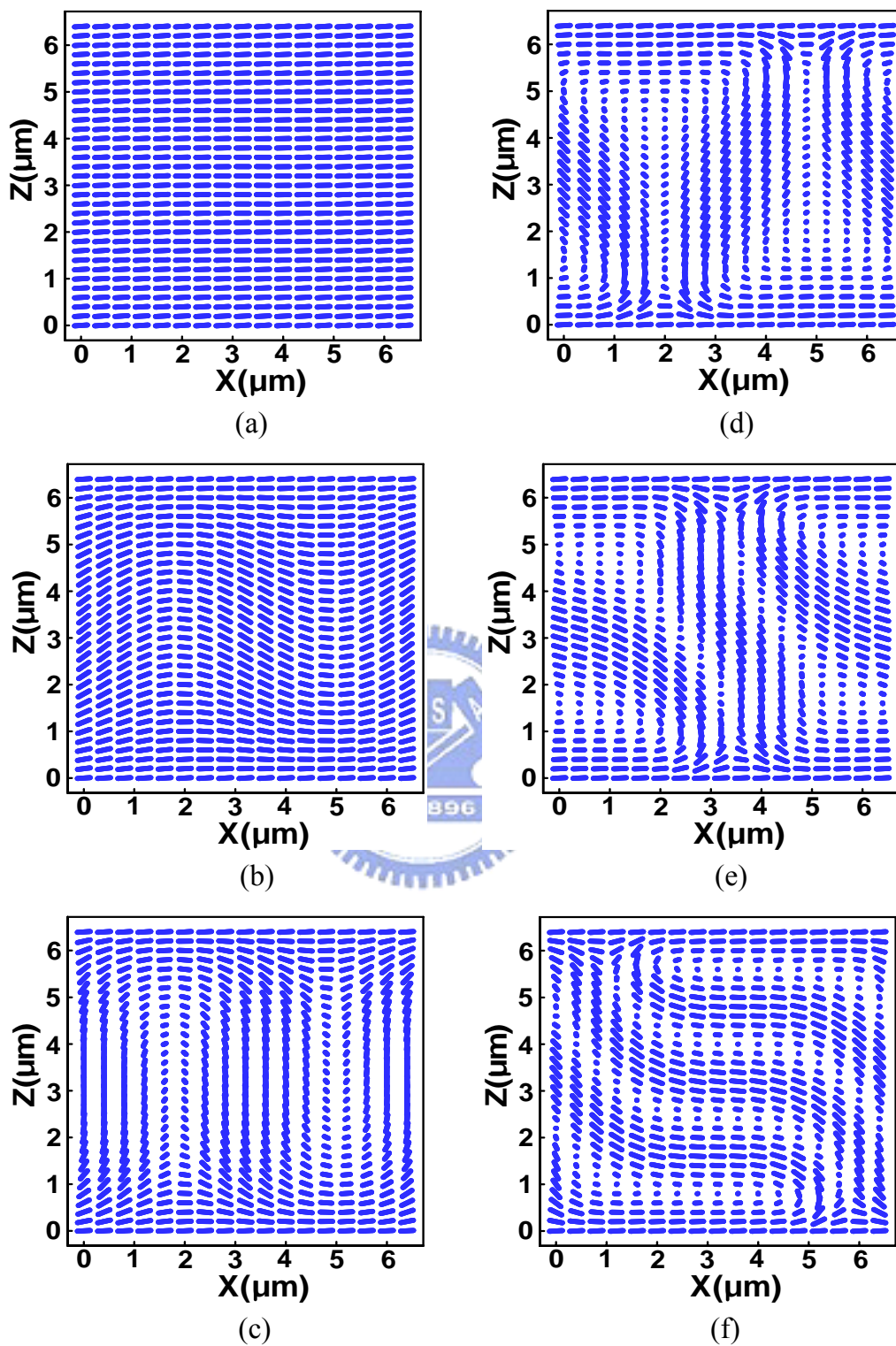
Figure 5.2 Simulated director configurations during the relaxation from the field-induced homogeneous texture to planar texture. Times are (a) 0.2 ms, (b) 100 ms, (c) 110 ms, (d) 250 ms, (e) 700 ms, (f) 1500 ms.

B. Homeotropic-planar relaxation

In this case, we investigated the relaxation of a cholesteric liquid crystal from the homeotropic texture in which the natural twist has been completely removed through the application of an electric field parallel to the helical axis, as shown in Fig. 5.3(a). When the electric field is turned off from the homeotropic texture, the ChLC molecules first go through a one-dimensional conical relaxation to the transient planar texture, as shown in Fig. 5.3(b). The transient planar state is a metastable state with the effective pitch $P^* = (K_{33} / K_{22})P_0$ [15-17]. As expected, we have one full 360° twist in the transient planar state ($d/P^* = 0.76$). Due to the frustration caused by the competition between the chirality and boundary constraints, the ChLC molecules proceed through a Helfrich undulation, as shown in Fig. 5.3(c), during the transition from transient planar texture to planar texture. We find that the wavelength of Helfrich undulation also matches well with the theoretical value in eq. (7) and this has been experimentally confirmed [16]. As can be seen from Fig. 5.3(d), the modulation increased in amplitude as the simulation progresses and then the ends of "fingers" mushroom out horizontally, as shown in Fig. 5.3(e). Figure 5.3(f) shows the equilibrium state with natural pitch and domain boundary. As expected, there are two full 360° twists in the equilibrium region. ($d/P_0 = 2.15$).
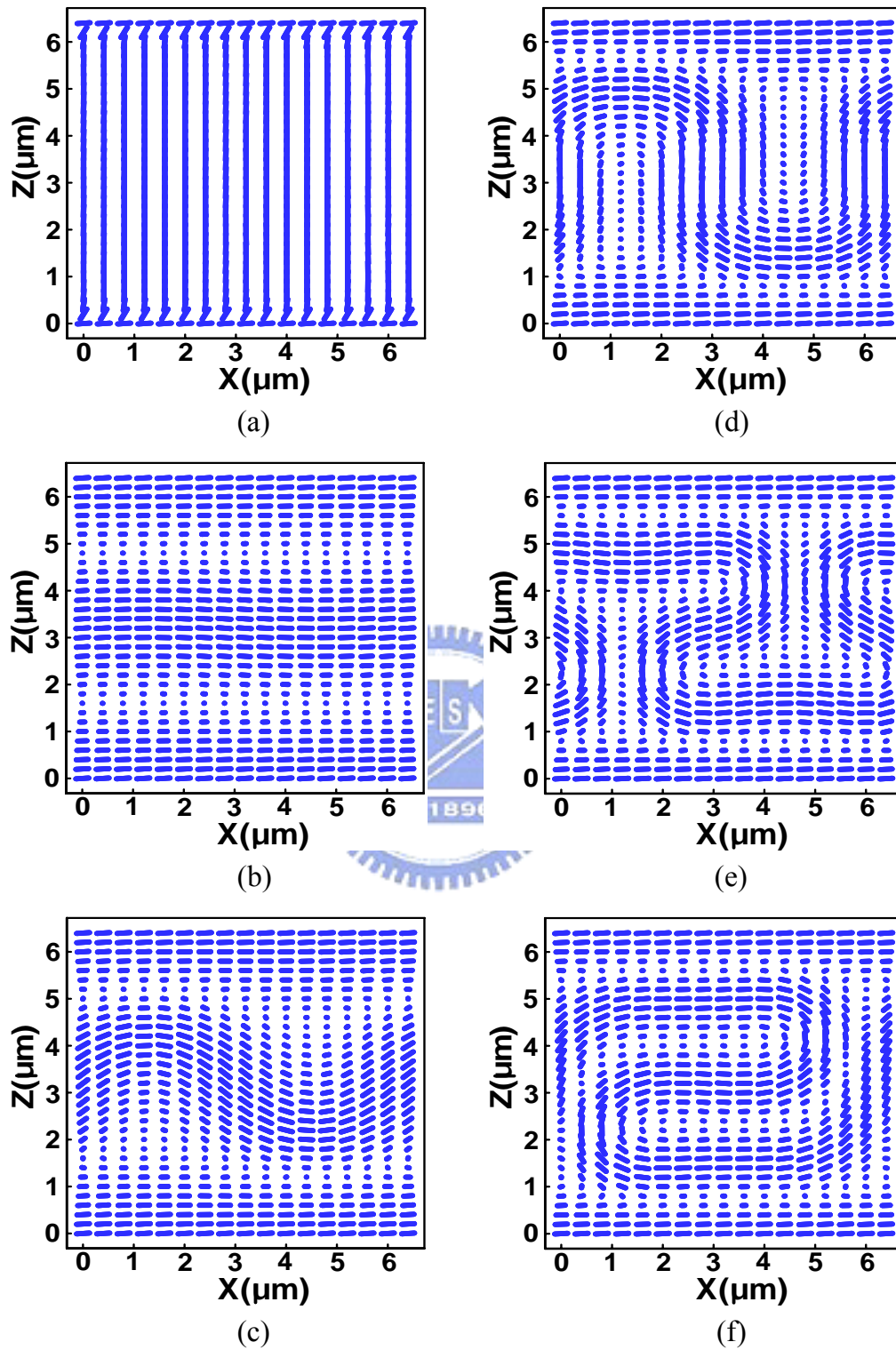
Figure 5.3 Simulated director configurations during the relaxation from the field-induced homeotropic texture to planar texture. Times are (a) 0.2 ms, (b) 365 ms, (c) 600 ms, (d) 765 ms, (e) 880 ms, (f) 1300 ms.

5.4 Discussion and conclusions

Figures 5.2 and 5.3 show the complete dynamic relaxation processes from the field-induced homogeneous and homeotropic textures, respectively to the stable planar texture. From the viewpoint of energy in a cholesteric liquid crystal system, because the homogeneous texture and transient planar texture are all metastable states, the stored twist energy in these two states are higher than the ground state (planar texture). This leads to the instability of the system and the elastic-induced Helfrich deformation occurs in order to alleviate the high twist energy.

The random noise which is conceived of a thermal fluctuation of the director plays an important role for the occurrence of Helfrich deformation. If this random fluctuation is not employed in the simulation, the ChLC molecules will relax to a metastable state and remain there. On the other hand, the formation process of Helfrich deformation is a nucleation process. Therefore, it takes a long time to initiate the Helfrich deformation, as shown in Figs. 5.2(a)-5.2(b) and Figs. 5.3(b)-5.3(c). However, the stored twist energy in the homogeneous texture is higher than that in the transient planar texture. Thus, the time to initiate the Helfrich deformation in the homogeneous texture is shorter than that in the transient planar texture.

The dynamic relaxation process of a field-unwound cholesteric liquid crystal has been well described by our model. The relaxation from the field-induced homogeneous texture to stable planar texture is in a sequence of the homogeneous-planar texture transition. However, the relaxation from the field-induced homeotropic texture to stable planar texture is in a different sequence of the homeotropic-transient planar-planar texture transition. These relaxation processes occur via an elastic-induced Helfrich deformation without introduction of

defects, which continuously converts into a stable planar texture with natural pitch and domain wall.

Based on our simulation results, we can conclude that an elastic-induced Hefrich deformation may be driven by the nonequilibrium layer spacing, induced either by external fields or mechanical strain fields or temperature variations, to increase the number of layers in a ChLC. In these situations, the structure of cholesteric layers favored by chirality can be achieved without the introduction of any defects.

References

[1] P. G. de Gennes: "Calcul de la distorsion d'une structure cholesterique par un champ magnetique" *Solid State Commun.* **6** 163 (1968).

[2] R. B. Meyer: "Effects of electric and magnetic fields on the structure of cholesteric liquid crystals" *Appl. Phys. Lett.* **12** 281 (1968).

[3] R. Dreher: "Remarks on the distortion of a cholesteric structure by a magnetic field" *Solid State Commun.* **13** 1571 (1973).

[4] S. V. Belyaev and L. M. Blinov: "Step unwinding of a spiral in a cholesteric liquid crystal" *Soviet Phys. JETP Lett.* **30** 99 (1979).

[5] M. Warner, E. M. Terentjev, R. B. Meyer and Y. Mao: "Untwisting of a cholesteric elastomer by a mechanical field" *Phys. Rev. Lett.* **85** 2320 (2000).

[6] W. Helfrich: "Deformation of cholesteric liquid crystals with low threshold voltage" *Appl. Phys. Lett.* **17** 531 (1970).

[7] J. P. Hurault: "Static distortions of a cholesteric planar structure induced by magnetic or ac electric fields" *J. Chem. Phys.* **59** 2068 (1973).

[8] V. G. Chigrinov, V. V. Belyaev, S. V. Belyaev and M. F. Grebenkin: "Instability of cholesteric liquid crystals in an electric field" *Sov. Phys. JETP* **50** 994 (1979).

[9] R.D. Kamien, and J. V. Selinger: "Order and frustration in chiral liquid crystals" *J. Phys. Condens. Matter* **13** R1 (2001).

[10] C. J. Cerritsma and P. Van Zanten: "Periodic perturbations in the cholesteric plane texture" *Phys. Lett. A* **37** 47 (1971).

[11] P. G. Gennes and J. Prost, *The Physics of Liquid Crystals* (Oxford University Press, New York, 1993) 2nd ed.

[12] P. Watson, J. E. Anderson and P. J. Bos: "Twist-energy-driven Helfrich modulations in cholesteric liquid crystals illustrated in the transient-planar to planar transition" *Phys. Rev. E* **62** 3719 (2000).

[13] I. A. Yao, J. J. Wu and S. H. Chen: "Three-dimensional simulation of the homeotropic to planar transition in cholesteric liquid crystals using the finite elements method" *Jpn. J. Appl. Phys.* **43** 705 (2004).

[14] E. Niggemann and H. Stegemeyer: "Magnetic field-induced instabilities in cholesteric liquid crystals: periodic deformations of the Grandjean texture" *Liq. Cryst.* **5** 739 (1989).

[15] M. Kawachi and O. Kogure "Hysteresis behavior of texture in the field-induced nematic-cholesteric relaxation" *Jpn. J. Appl. Phys.* **16** 1673 (1977).

[16] P. Watson, J. E. Anderson, V. Sergan and P. J. Bos: "The transition mechanism of the transient planar to planar director configuration change in cholesteric liquid crystal displays" *Liq. Cryst.* **26** 1307 (1999).

[17] D.-K. Yang and Z.-J. Lu: "Switching mechanism of bistable reflective cholesteric displays" *SID 95 Dig. Tech. Pap.* **26** 351 (1995).

Chapter 6

Electric-Field-Induced Modulated Textures during the Planar to Focal Conic Texture Transition

We observed the modulated textures in a planar-aligned cholesteric liquid crystal cell by applying an electric field parallel to its helical axis. In this system, the twist favored by the chirality competes with the applied electric field. This competition causes the system to develop a series of ordered textures, in the sequence of striped texture-hexagonal texture-striped texture, with the increase of electric field. Of these textures, the hexagonal texture was experimentally observed for the first time.

6.1 Introduction

A cholesteric liquid crystal (ChLC) is a nematic liquid crystal composed of optically active molecules. Such a structure can also be obtained by doping a small quantity of chiral molecules into a nematic liquid crystal. The chiral molecules possess a characteristic of chirality that induces liquid crystal molecules to twist. However, when the twist favored by the chirality competes with geometric constraints or with an applied electric or magnetic field, the ChLC system becomes instable and the ordered modulated textures appear [1,2].

The mechanisms of ordered pattern formation can be classified into two types according to the cause of the modulation [3]. One is the elastic-driven modulation. Under this condition, the system is frustrated due to the competition between the chirality, which favors a twist deformation in the molecular orientation, and boundary constraints, which favor the alignment of molecules along the surfaces of the ChLC cell [4-6]. The other is the field-driven modulation. Under this condition, the system is frustrated because of the competition between the chirality, which favors a twist modulation in the molecular orientation, and the electric field, which favors the alignment of molecules along the direction of the electric field [7].

An example of an elastic-driven striated modulation was observed during the relaxation of a electric-field-unwound cholesteric liquid crystal [4,5]. An electric-field-driven striated modulation in ChLC cells was first theoretically investigated by Helfrich [8] and refined by Hurault [9] and Chigrinov et al. [10]. Hinshaw et al. studied the structures of modulated textures in thin films composed of tilted chiral molecules [11]. By considering all the orders of Landau expansion, they predicted that either a striped texture with parallel defect walls, as shown in Fig. 6.1, or a hexagonal texture containing disclinations and intersectional defect walls, as shown in Fig. 6.2, can occur. However, the hexagonal texture has not been observed [1]. In this chapter, we focused on the observation of electric-field-driven modulations in chiral nematic liquid crystals and investigated the transformations between ordered textures, such as that between a striped texture and a hexagonal texture, by changing the applied electric field.
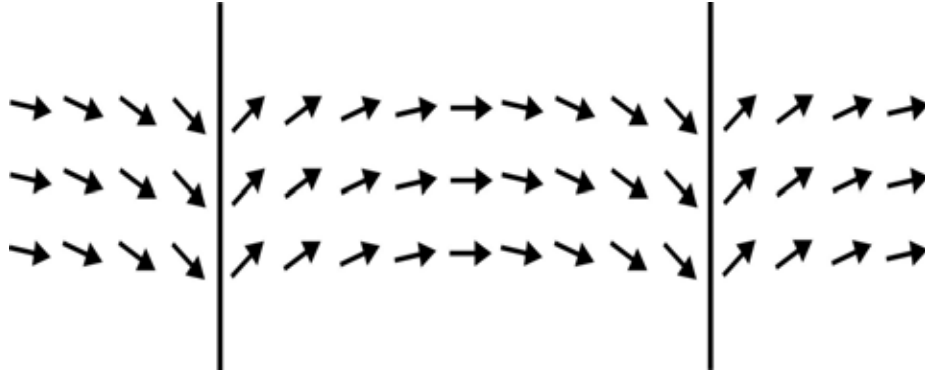
Figure 6.1 Striped texture separated by long domain walls. Adapted from ref. 11.
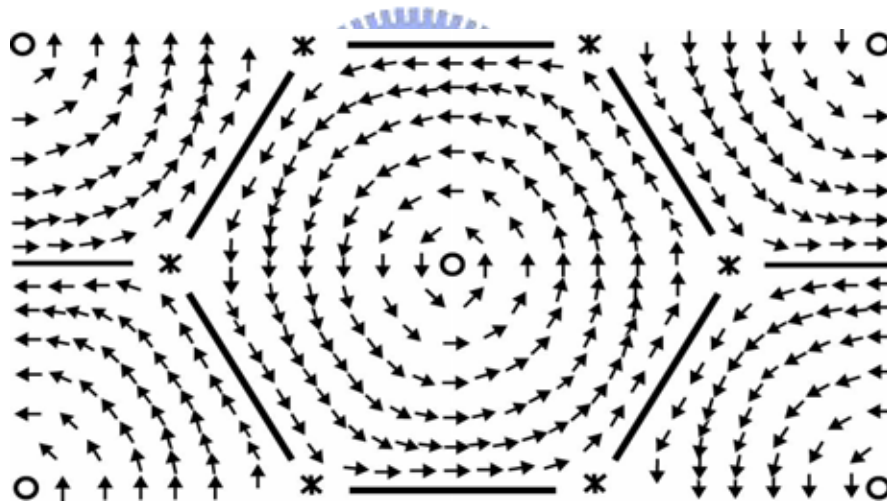

Figure 6.2 Hexagonal texture separated by domain walls and +1 and −1/2 disclinations. This structure has +1 disclinations at the center of the domains and −1/2 disclinations at corners. Adapted from ref. 11.
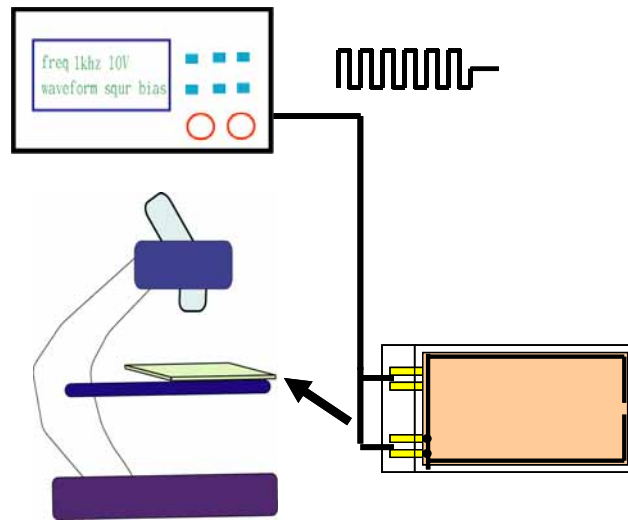
Figure 6.3 Experimental setup to observe the electric-field-induced ordered textures in cholesteric liquid crystal cells.

6.2 Sample preparation and experimental setup

The liquid crystal used was a mixture of 97% ZLI-4792 (Merck Co.) doped with 3% chiral additive S811 (Merck Co.), which resulted in a quiescent pitch $P_0 = 2.98$ μm. The liquid crystal (ZLI-4792) possesses a positive dielectric anisotropy $\Delta\varepsilon = 5.2$ (1 kHz) and elastic constants K11 = 13.2 pN, K22 = 6.5 pN, K33 = 18.3 pN for splay, twist and bend deformations, respectively. The cell consisted of two glass plates coated with SE-3310 (Nissan Co.) polyimide which provided a planar alignment layer. The polyimide was rubbed to give a pretilt angle of approximately 4°. The cell was assembled such that the rubbing directions of the layers were antiparallel, and the cell gap was measured to be 6.4 μm by an interferometer. Hence, the thickness-to-natural-pitch ratio (d/P_0) was 2.15. The pattern formation of a ChLC was observed under a polarizing microscope, applying a 1 kHz square wave to the sample. The experimental setup is shown in Fig. 6.3.
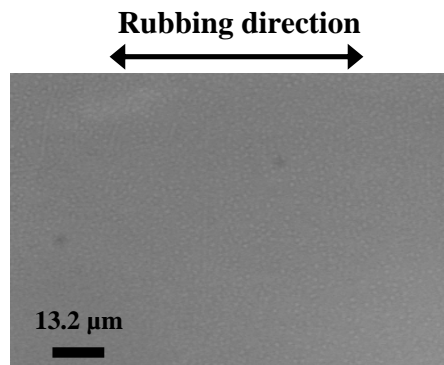
Rubbing direction

13.2 μm

Figure 6.4 Microphotograph of a planar texture.

6.3 Ordered textures

Consider a cholesteric liquid crystal initially in a planar texture, as shown in Fig. 6.4. When the electric field, applied parallel to the helical axis of the planar texture, competed with the chirality, the system became instable. In response to this instability, the system first underwent a sinusoidal deformation along the rubbing direction at 4.73 V_{rms}. Hence, the direction of the stripes was approximately perpendicular to the rubbing direction, as shown in Fig. 6.5. On increasing the voltage, the amplitude of the undulation perpendicular to the rubbing direction increased and the system formed a hexagonal texture at 4.98 V_{rms}, as shown in Fig. 6.6. Each hexagonal lattice possessed unequal wall angles and wall lengths. With further increase of the voltage, the hexagonal texture transformed into an ordered striped texture again at 5.41 V_{rms}, as shown in Fig. 6.7. However, the period of this striped texture was half of that shown in Fig. 6.5 and was measured to be approximately 6.6 μm.

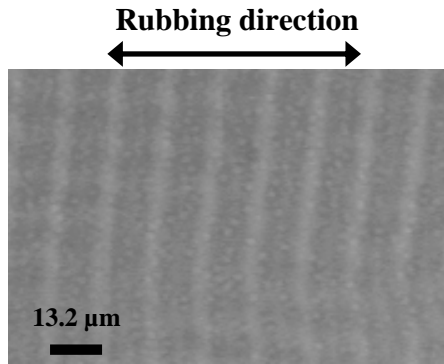**Rubbing direction**

13.2 μm

Figure 6.5 Microphotograph of a striped texture. The period of the stripes is 13.2 μm.

Rubbing direction

13.2 μm
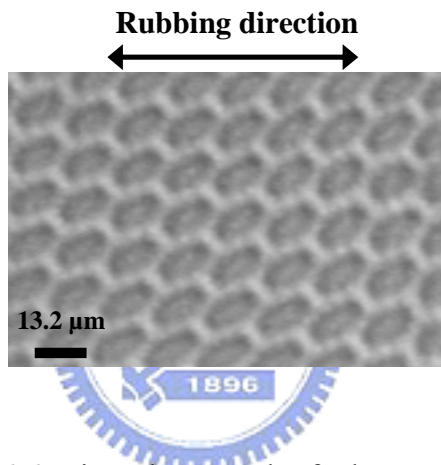
Figure 6.6 Microphotograph of a hexagonal texture.
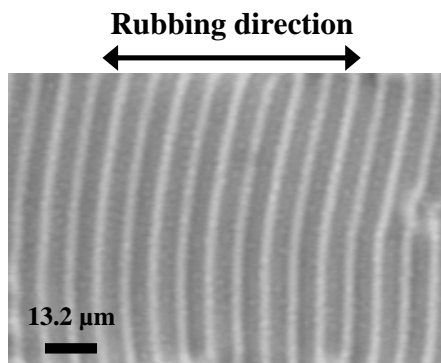

Rubbing direction

13.2 μm

Figure 6.7 Microphotograph of a striped texture. The period of the stripes is 6.6 μm.

91

6.4 Conclusions

In summary, we experimentally observed the texture transformations in a ChLC system under a weak electric field. When the chirality of the system was frustrated, it may develop spatially ordered textures. The appearance of a specific ordered texture will depend on the chirality (which is inversely proportional to the pitch) of the system and the applied fields. The chirality of the system will force the liquid crystal molecules to remodulate with increasing electric field in order to alleviate the increase of the dielectric energy of the system. Hence, complex and interesting ordered textures appear with increasing electric field. In this experiment, either a one-dimensional ordered striped texture or a two-dimensional ordered hexagonal texture was obtained depending on the applied electric-field strength. A similar two-dimensional grid texture has been observed in a ChLC with a large pitch P_0 [7]. Of these textures, the hexagonal texture was first experimentally observed.

References

[1] R. D. Kamien and J. V. Selinger: "Order and frustration in chiral liquid crystals" *J. Phys. Condens. Matter* **13** R1 (2001).

[2] P. Oswald, J. Baudry and S. Pirkl: "Static and dynamic properties of cholesteric fingers in electric field" *Phys. Rep.* **337** 67 (2000).

[3] P. G. de Gennes and J. Prost: *The Physics of Liquid Crystals* (Clarendon Press, Oxford, 1993) 2nd ed., p. 361.

[4] P. Watson, J. E. Anderson and P. J. Bos: "Twist-energy-driven Helfrich modulations in cholesteric liquid crystals illustrated in the transient-planar to planar transition" *Phys. Rev. E* **62** 3719 (2000).

[5] S. V. Belyaev and L. M. Blinov: "Step unwinding of a spiral in a cholesteric liquid crystal" *JETP Lett.* **30** 99 (1979).

[6] E. Niggemann and H. Stegemeyer: "Magnetic field-induced instabilities in cholesteric liquid crystals: periodic deformations of the Grandjean texture" *Liq. Cryst.* **5** 739 (1989).

[7] L. M. Blinov and V. G. Ghigrinov: *Electrooptic Effects in Liquid Crystals* (Springer-Verlag, New York, 1994) p. 319.

[8] W. Helfrich: "Deformation of cholesteric liquid crystals with low threshold voltage" *Appl. Phys. Lett.* **17** 531 (1970).

[9] J. P. Hurault: "Static distortions of a cholesteric planar structure induced by magnetic or ac electric fields" J. Chem. Phys. **59** 2068 (1973).

[10] V. G. Chigrinov, V. V. Belyaev, S. V. Belyaev and M. F. Grebenkin: "Instability of cholesteric liquid crystals in an electric field" *Sov. Phys.*

JETP **50** 994 (1979).

[11] G. A. Hinshaw, Jr., R. G. Petschek and R. A. Pelcovits: "Modulated phases in thin ferroelectric liquid-crystal films" *Phys. Rev. Lett.* **60** 1864 (1988).

Chapter 7

Electrically Controllable Cholesteric Liquid Crystal Phase Gratings

In suitable condition, the homeotropic aligned cholesteric liquid crystal cell can be in fingerprint texture when abruptly switching off the applied electric field. The striped orientation depends not only on the thickness-to-pitch (d/P_0) ratio, but also on the applied driving voltage. In this chapter, the cholesteric liquid crystal phase grating with the field-controllable grating orientation and grating period is realized and the operational mechanism of this device is presented.

7.1 Introduction

In cholesteric liquid crystals, the liquid crystal molecules rotate in space about their helical axis. This periodic helical structure leads to very specific optical properties which are determined by the pitch length and the arrangement of the helical axis of cholesteric liquid crystals. When the helical axis is perpendicular to the glass surfaces, the Bragg reflecting planar texture is obtained. When, on the other hand, the helical axis is parallel to the glass surfaces, the diffractive fingerprint texture is obtained.

Under the application of an electric field, if the field is higher than a critical value and the material has a positive dielectric anisotropy, the helical structure is

unwound to a homeotropic texture. The threshold voltage is denoted as V_{fh}. If the applied voltage is decreased below another threshold voltage V_{hf}, the cholesteric liquid crystals relax to the fingerprint texture. $V_{fh} > V_{hf}$ and their difference is called hysteresis [1].

In recent years, the planar-aligned fingerprint-type cholesteric liquid crystal phase gratings confined between two parallel substrates have been extensively studied, both theoretically and experimentally [2-9]. The fingerprint texture can be obtained by applying an electric field parallel to the helical axis of a planar-aligned cell. As the fingerprint texture is formed, the period is tuned by changing the applied electric field [3]. However, the fingerprint texture is not stable when the applied electric field is removed [5]. On the other hand, our previous experimental evidence has shown that the planar-aligned cholesteric liquid crystal cell has no more than two possible striped directions in the fingerprint texture [9,10]. The striped direction is determined by the rubbing direction and d/P_0 ratio. In this chapter, the electrically switchable cholesteric liquid crystal phase grating including both grating orientation and grating period is realized by applying a suitable driving waveform to a homeotropic-aligned cholesteric liquid crystal cell with patterned electrode configurations. Moreover, the diffractive effect of this device is studied [2,3].

7.2 Sample preparations and experimental setups

The cholesteric liquid crystal cells were composed of two glass substrates. Each possesses two patterned 1cm×1cm square indium tin oxide (ITO) electrodes, as shown in Fig. 7.1. The glass substrates with patterned ITO electrodes were coated with polyimide (JALS-2021) for homeotropic alignment and were rubbed unidirectionally to provide an inplane "easy axis" of the molecular orientation. The plastic pearl balls with 6-μm diameter were spread to maintain the cell gap and the

cells were assembled such that the rubbing directions were antiparallel. After the cell was assembled, the cell gap was measured to be d = 6 ± 0.1 µm by an interferometer. The cells were then filled with the cholesteric material obtained by doping the nematic E7 with the chiral agent S811 (both purchased form Merck Co.). After the injection of the chiral mixture, the cell was sealed with AB sealant. In this work, we fabricated two typical homeotropic-aligned cholesteric liquid crystal cells with the same cell gap but different weight concentration of the chiral additive. The d/P_0 ratios are 2.05 and 1.83 for cell 1 and cell 2, respectively.

The pattern formation of cholesteric liquid crystal cells was observed under the polarizing microscope. The applied voltage was in the form of a 1 kHz square wave generated by an arbitrary waveform generator and the square wave was routed through a linear amplifier. The experimental setup is shown in Fig. 7.2. On the other hand, the diffractive characteristics of these cells were studied. When a He-Ne laser light was normally incident on the cell, the light will be diffracted and the diffracted beams can be steered by changing the applied voltage. Figure 7.3 shows the experimental setup of the diffraction.
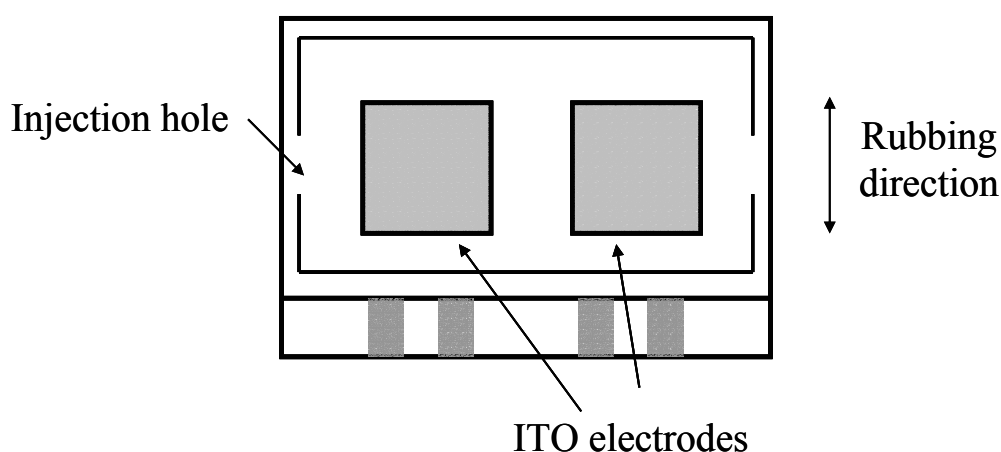
Figure 7.1 Schematic diagram of the cell structure with two 1cm×1cm square ITO electrodes on each glass substrate.
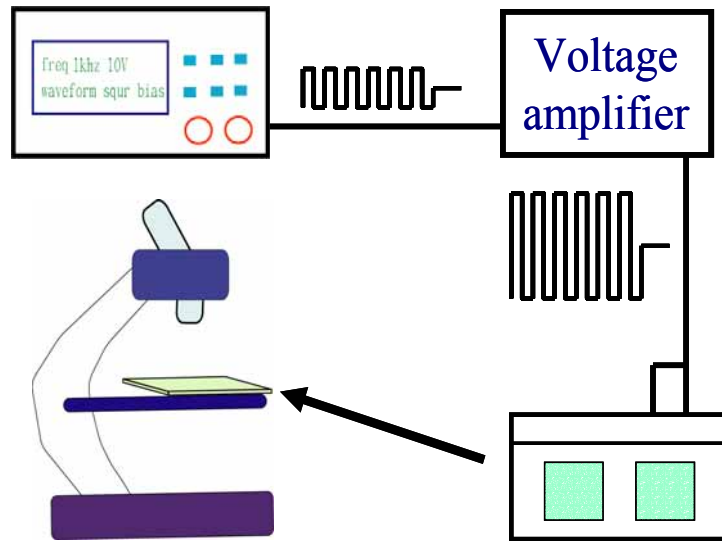
97

Figure 7.2 Experimental setup to observe the pattern formation in cholesteric liquid crystal cells.
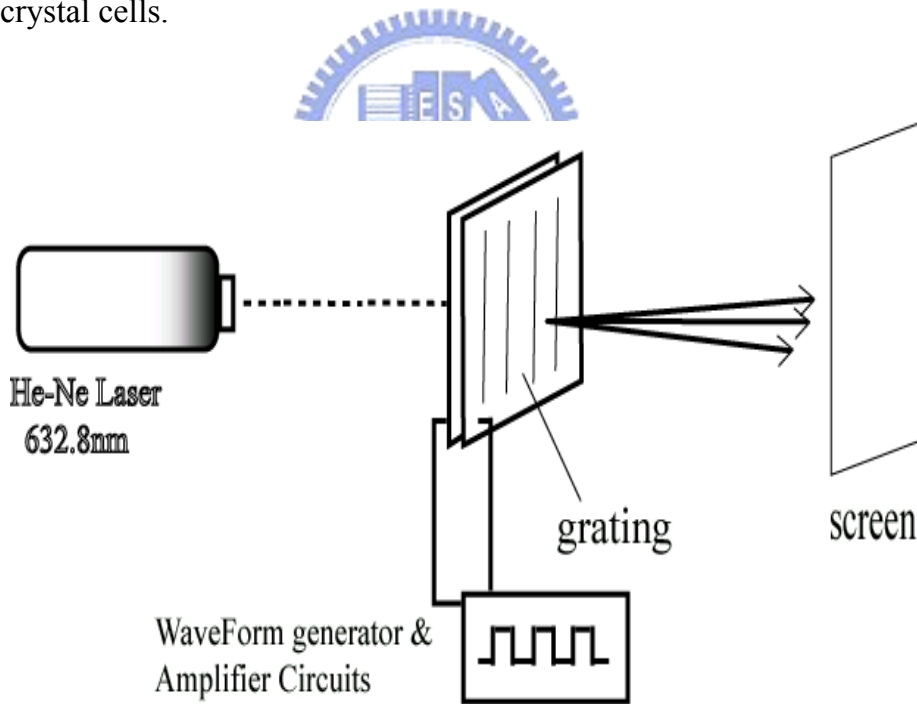

Figure 7.3 Experimental setup of the diffraction.

7.3 Mechanisms of the pattern formation

When the cell is initially prepared, the multidomain fingerprint texture is obtained. The homeotropic texture can be obtained by applying an AC voltage (1 kHz) to the cell. The unwinding voltage for cell 1 and cell 2 are 3.42 V_{rms} and 2.2 V_{rms}, respectively. This consists with that the threshold voltage V_{fh} increases with the d/P_0 ratio [9]. In this situation, the cholesteric liquid crystal molecules inside the square electrodes are in a homeotropic texture, while the cholesteric liquid crystal molecules in the fringe region (outside the square electrodes) are not fully unwound because of the weak fringe field. Hence, the fingerprint texture with stretched pitch is formed in the fringe region. When the fringe field is further increased, the cholesteric liquid crystal molecules in the fringe region will be further unwound and the dark region observed under cross polarized microscope expands. Once the voltage is switched off abruptly, the cholesteric liquid crystal molecules inside the electrodes temporarily remain in the homeotropic texture due to the hysteresis of cholesteric liquid crystals. However, the partially unwound cholesteric liquid crystal molecules in the fringe region first relax to the fingerprint texture and then induce the fast stripe formation form the edges to the center of electrodes.

We classify the striped textures into two types, according to the striped arrangement. One is the radiant type stripe (RTS) in which the striped orientation radiates from the texture center, as shown in Fig. 7.4(a). The other is the concentric type stripe (CTS) in which the striped orientation circles the texture center, as shown in Fig. 7.4(b). In this experiment, RTS and CTS are obtained for cell 1 and cell 2, respectively.
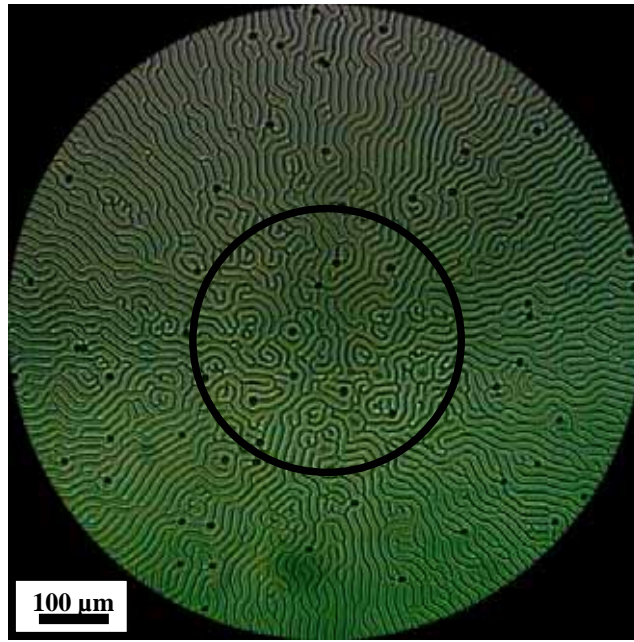
(a)
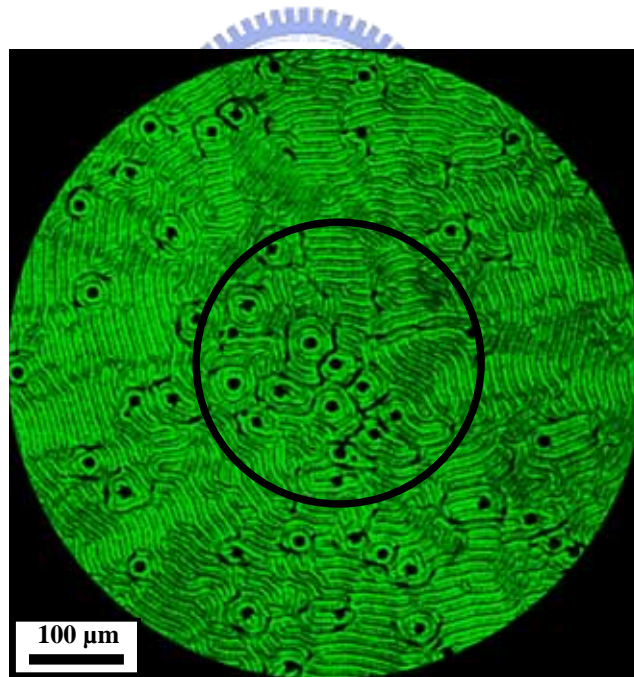
(b)

Figure 7.4 Polarized microscope striped textures. (a) Radiant type stripe ($d/P_0 = 2.05$); (b) Concentric type stripe ($d/P_0 = 1.83$). The circles in both two figures indicate the texture centers.
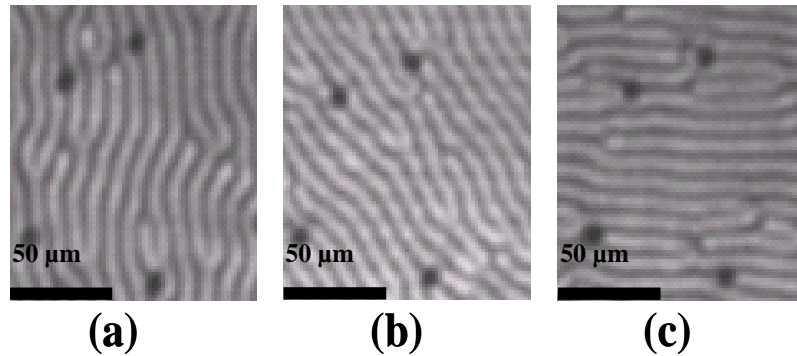
Figure 7.5 Observed striped directions at different applied voltage for cell 1. (a) 30 V_{rms}, (b) 13 V_{rms}, (c) 2.5 V_{rms}.

7.4 Controllable striped orientation

In this experiment, the striped formation is observed by applying a voltage (witch is larger than V_{fh}) for 10 s and then switching off it. Here and below, we observe the striped formation under the above conditions but only change the applied voltage. Figures 7.5(a-c) illustrate how the applied voltage changes the striped orientation for cell 1. The applied voltage are 30 V_{rms}, 13 V_{rms} and 2.5 V_{rms}, respectively and the angles between the rubbing direction and the striped direction are about 90°, 45° and 0°, respectively. These stripes are stable for several months. The same results are obtained for cell 2. For convenient, we define the angle between the striped orientation at some applied voltage and that at 30 V_{rms} as the deviation angle. Figure 7.6 shows the measured deviation angle as a function of applied voltage. It is obvious that the deviation angle decreases with the applied voltage and is independent of the types of stripes (CTS or RTS).
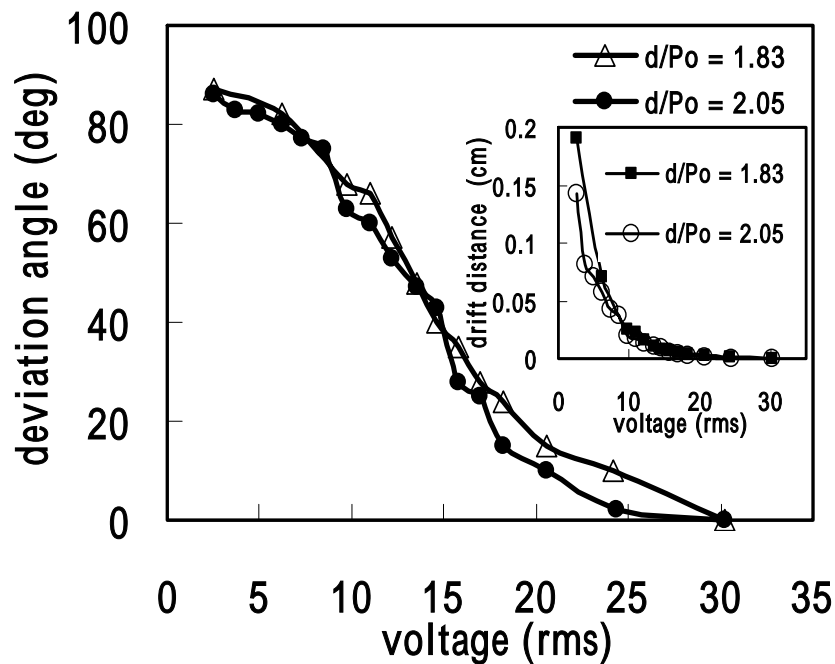
101

Figure 7.6 The deviation angle vs. applied voltage for cell 1 (d/P_0 = 2.05) and cell 2 (d/P_0 = 1.83). The insert shows the drift distance of the texture centers as a function of applied voltage.

7.5 Operational mechanism

The mechanism of the rotation of stripes is resulting from the drift of the texture center. The insert of Fig. 7.6 shows the relationship between the drift distance of the texture center and the applied voltage. The drift distance is measured with respect to the location of the texture center at 30 V_{rms} and decreases with the applied voltage. Figures 7.7(a-b) and Figs. 7.7(c-d) show the schematic diagrams of the rotation of stripes for cell 1 and cell 2, respectively, as the texture centers drift with applied voltage. However, the reason for the drift of the texture center is caused by the surface rubbing direction. To confirm the above interpretation, we fabricated a cell using the same conditions with cell 2 except that the alignment layer is unrubbed.
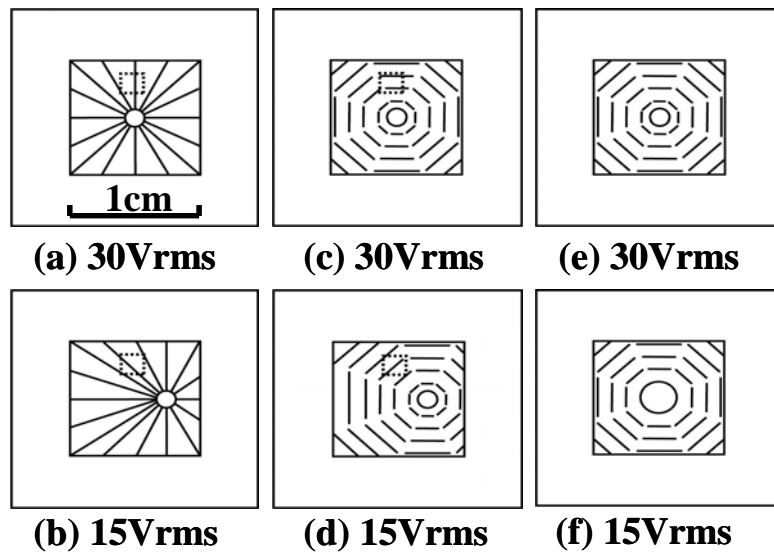
Figure 7.7 Schematic diagram of the rotation of stripe as the texture centers drift with applied voltage: (a) and (c) show the schematic diagrams of RTS and CTS, respectively; (b) and (d) show the drift of texture center for RTS and CTS, respectively; (e) and (f) show that the texture center of unrubbed cell is fixed with applied voltage. The stripe direction observed in the dashed square rotates with applied voltage.

In an unrubbed cell, the mediating velocity of the fringe-field-induced homeotropic to fingerprint (H-F) texture transition is the same for each side of square electrodes. Therefore, the location of the texture center does not drift in the unrubbed cell while the size of the texture center decreases with the applied voltage, as shown in Figs. 7.7(e-f). When the cell is rubbed, the effect of the lateral field of the fringe field parallel to the rubbing direction on the mediating velocity of the H-F texture transition is different to that perpendicular to the rubbing direction. In other words, this rubbing direction destroys the symmetric mediating velocity of H-F texture transition and results in the movement of the texture center. Because the mediating velocity of the H-F texture transition increases with the fringe field, we can make use of that to control the drift velocity of the texture center along one direction which is caused by the rubbing direction.
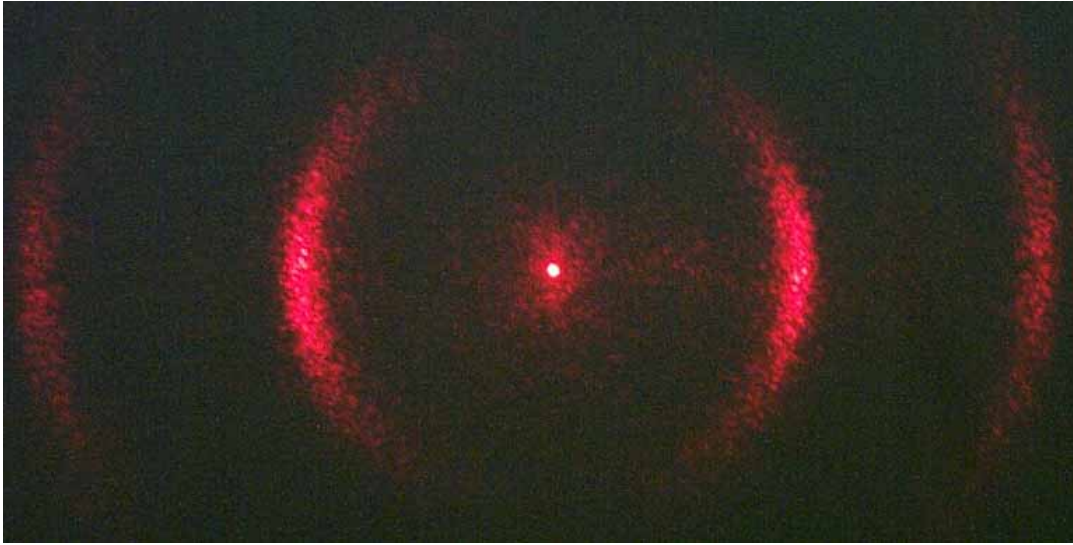
Figure 7.8 Arc-shaped diffracted beams for cell 1

7.6 Controllable striped period

The formation of the gratings can be classified into two types. One is the so-called developable-modulation (DM) type. For this type of gratings, the stripes appear in a manner similar to the development of a photographic image. The other is growing-modulating (GM) type. For this type of gratings, the stripes are initiated near the edges and defects, and then slowly extend to the whole sample. On the other hand, the shapes of the diffracted beams for these two types of gratings are different. The shape of the diffracted beams for the regular DM type grating is circular. However the shape of diffracted beams for the GM type grating is arc-shaped [8]. In this chapter, the gratings we obtained belong to the GM type gratings. Although the stripes are not uniform, the diffracted beams can still be steered. In our experiment, the laser light is incident on a location which is between the edge of electrodes and the texture center, as shown in Fig. 7.7. Figure 7.8 shows the arc-shaped diffracted beams for cell 1 when the applied bias voltage is 1 V_{rms}.

For a cholesteric liquid crystal cell, the relationship between the pitch (striped period) and the applied voltage is obtained by measuring the first-order diffraction angle with respect to the applied voltage. The first-order diffraction angle is obtained by measuring the distance from the zero-order diffraction spot to the fist-order arc-shaped diffraction spot with the maximum intensity. The pitch of a cholesteric liquid crystal system will increase with the applied voltage. This results in the decrease of the first-order diffraction angle with the applied voltage. Figure 7.9 shows the relationship between the first-order diffraction angle and the applied voltage for a beam (He-Ne laser) incident normally to the films with various d/P_0 ratios. As the incident beam is fixed, a variation of applied voltage results in a continuous deflection of the diffracted beams. The striped period elongated to infinity when the voltage increased to the cholesteric-to-nematic phase transition voltage V_{fh} [11].
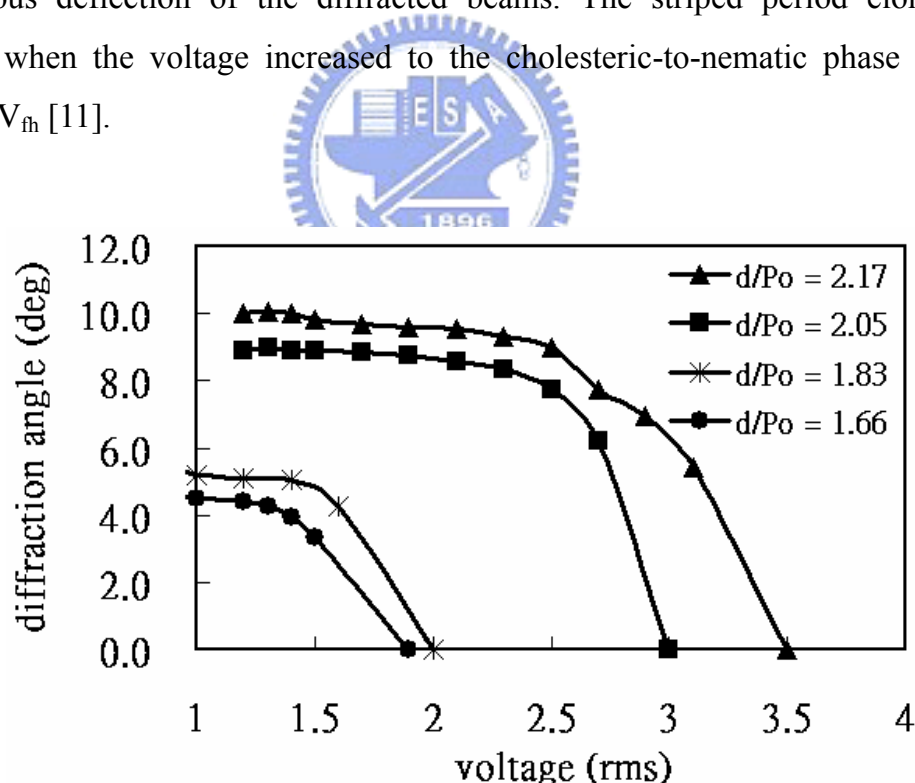

Figure 7.9 The first order diffraction angle as a function of applied voltage. Films with $d/P_0 = 2.17$ and $d/P_0 = 2.05$ are radiant type stripes. Films with $d/P_0 = 1.83$ and $d/P_0 = 1.66$ are concentric type stripes.
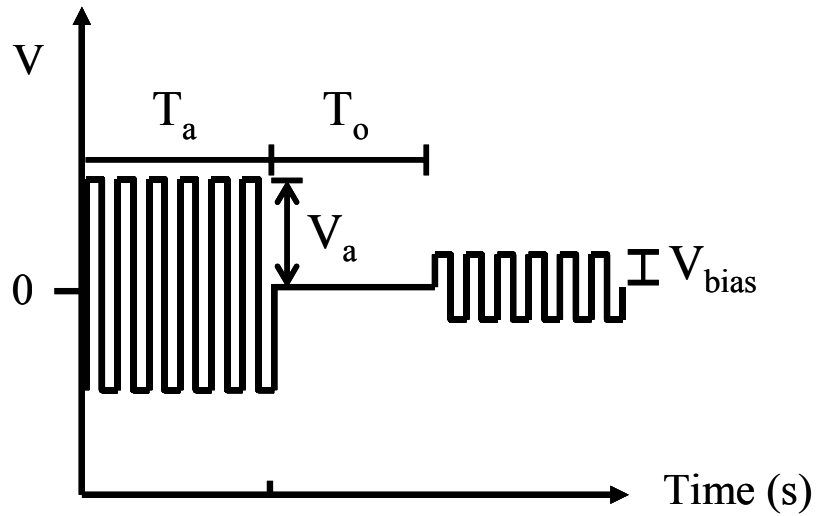
105

Figure 7.10 The driving waveform of cholesteric liquid crystal phase gratings.

7.7 Driving scheme

There are two types of stripes in homeotropic aligned cholesteric liquid crystal films with patterned electrode configurations. The striped orientation and striped period of each type of stripes can be electrically controlled, respectively. This device provides a potential application in the electro-optical switching of the gratings and optical information processing. On the basis of the understandings for the striped formation and the operational mechanism of the cholesteric liquid crystal phase gratings, we design a driving waveform, as shown in Fig. 7.10, to drive these devices. As can be seen from Fig. 7.6, the striped orientation can be controlled by applying a voltage V_a to the cell for a time T_a, and then switching off it. T_o is the time required for the striped formation. Once the stripe is formed, the striped period can be tuned by applying a bias voltage V_{bias}. In this experiment, we let $T_a = T_o = 10$ s.

References

[1] Y.-M. Zhu and D.-K. Yang: "Observation of pattern evolution during homeotropic-focal conic transition in cholesteric liquid crystals" *Phys. Rev. Lett.* **82** 4855 (1999).

[2] D. Subacius, P. J. Bos and O. D. Lavrentovich: "Switchable diffractive cholesteric gratings" *Appl. Phys. Lett.* **71** 1350 (1997).

[3] D. Subacius, S. V. Shiyanovskii, P. J. Bos and O. D. Lavrentovich: "Cholesteric gratings with field-controlled period" *Appl. Phys. Lett.* **71** 3323 (1997).

[4] C. M. Titus and P. J. Bos: "Efficient, polarization-independent, reflective liquid crystal phase grating" *Appl. Phys. Lett.* **71** 2239 (1997).

[5] S. N. Lee, L. C. Chien and S. Sprunt: "Polymer-stabilized diffraction gratings from cholesteric liquid crystals" *Appl. Phys. Lett.* **72** 885 (1998).

[6] C. V. Brown, E. E. Kriezis and S. J. Elston: "Optical diffraction from a liquid crystal phase grating" *J. Appl. Phys.* **91** 3495 (2002).

[7] C.-H. Lin, Y.-G. Fuh, T.-S. Mo and C.-Y. Huang: "Polymer-Stabilized Reflective Fingerprint Cholesteric Texture Grating" *Jpn. J. Appl. Phys.* **41** 7441 (2002).

[8] Y.-G. Fuh, C.-H. Lin and C.-Y. Huang: "Dynamic pattern formation and beam-steering characteristics of cholesteric gratings" *Jpn. J. Appl. Phys.* **41** 211 (2002).

[9] J.-J Wu, Y.-S. Wu, F.-C. Chen and S.-H. Chen: "Formation of phase grating in planar aligned cholesteric liquid crystal film" *Jpn. J. Appl. Phys.* **41** L1318 (2002).

[10] J.-J Wu, F.-C. Chen, Y.-S. Wu and S.-H. Chen: "Phase Gratings in pretilted homeotropic cholesteric liquid crystal films" *Jpn. J. Appl. Phys.* **41** 6108 (2002).

[11] P. G. de Gennes: "Calcul de la distorsion d'une structure cholesterique par un champ magnetique" *Solid State Commun.* **6** 163 (1968).

Chapter 8

Summery and Conclusions

In this dissertation, we have investigated the mechanisms of three types of texture transitions in planar-aligned cholesteric liquid crystal cells: homeotropic-planar texture transition, homogeneous-planar texture transition and planar-focal conic texture transition. In addition, the mechanism of the homeotropic-fingerprint texture transition is discussed in homeotropic-aligned cholesteric liquid crystal cells. The understandings for the mechanisms of texture transitions in cholesteric liquid crystals not only help us improving the driving schemes for the cholesteric displays but also make us to design new cholesteric phase gratings.

However, the mechanisms of the texture transitions are very complex because of the "irregular" transition processes. Therefore, in this thesis the finite element method and the relaxation method were first used to simulate the dynamics of texture transitions in cholesteric liquid crystals. Under the continuum theory, the "defect-free" texture transitions can be correctly simulated. The simulation was performed in three and two dimensions using unequal elastic constants and fixed boundary conditions.

The dynamics of the homeotropic-planar texture transition was numerically investigated in a planar-aligned cholesteric liquid crystal cells when the applied

electric field was turned off form the homeotropic texture. The simulation reproduced the observed relaxation from the homeotropic texture to the long-pitch transient planar texture. The simulation also agreed well with the suggestion that the transient planar-planar texture transition occurred via a three-dimensional Helfrich deformation without introduction of defect cores. Moreover, the transient planar-planar texture transition was a nucleation process which resulted in the long transition time. By monitoring the evolution of transient transmittance, the effects of bias waveforms on the homeotropic-planar texture transition were studied. We found that the long transition time can be improved by doping a number of impurities or applying a bias voltage during the transition from the transient planar texture to the maximum Helfrich deformation. The bias voltage can speed up the nucleation process in the transient planar texture and can increase the amplitude of Helfrich deformation.

Similarly, we also numerically investigated the dynamics of the transition from the field-induced homogeneous texture to planar texture. When the unwinding field was turned off abruptly, the relaxation process of a field-unwound cholesteric liquid crystal was accompanied by an elastic-induced Helfrich deformation without introduction of defects, which will continuously converts into a stable planar texture with an intrinsic pitch and domain wall. In a word, both transient planar-planar and homogeneous-planar texture transitions occurred via an elastic-induced Helfrich deformation. Therefore, we can conclude that an elastic-induced Helfrich deformation may be driven by the nonequilibrium layer spacing, induced either by external fields or mechanical strain fields or temperature variation, to increase the number of layers in cholesteric liquid crystals.

On the other hand, we have observed the modulated textures during the planar-focal conic texture transition under the weak electric field. When the chirality of the system suffers competing, it may develop spatially ordered textures. The appearance of a specific ordered texture will depend on the chirality of the system and the applied electric field. The chirality of the system forced the liquid crystal molecules to remodulate with increasing the electric field in order to alleviate the increase of the dielectric free energy of the system. In our experiment, either a one-dimensional ordered striped texture or a two-dimensional ordered hexagonal texture can be obtained. Of these textures, the hexagonal texture was experimentally observed for the first time.

Finally, we experimentally observed the stripe formation during the homeotropic-fingerprint texture transition in homeotropic-aligned cholesteric liquid crystal cells with patterned electrode configurations. When the unwound electric field was turned off abruptly, the fingerprint texture was quickly formed via a fast stripe formation from the edges to the center of square electrodes. There were two types of stripes formed depending on the d/P_0 ratio of the system. One was the radiant type stripe (RTS). The other was the concentric type stripe (CTS). By applying a suitable waveform, the striped orientation and striped period of each type of stripes can be electrically controlled, respectively. This device provides a potential application in the electro-optical switching of gratings and optical information processing.

Vita

- **Personal Information**（個人簡歷）**:**

Surname and First name in English and Chinese（中英文姓名）:

<u>I-An Yao　（姚怡安）</u>

Date and Place of Birth：　<u>Nov. 1th, 1976,　Yunlin, Taiwan</u>

Contact Address in English and Chinese（中英文地址）:

<u>No. 4-13, Sucuo Village, Liujiao Shiang, Chiayi County 615, Taiwan (R.O.C.).</u>
（嘉義縣六腳鄉蘇厝村 4 之 13 號）

Phone/Fax：　<u>03-5712121 ext. 56344 (phone)　/　03-5716631 (Fax)</u>

E-mail：<u>fishane.eo89g@nctu.edu.tw</u>

- **Academic degrees**（學歷）**:**

B.S.	1996.9~2000.6	Department of Physics, National Cheng Kung University（國立成功大學物理系）
M.S.	2000.9~2001.6	Institute of Electro-Optical Engineering, National Chiao Tung University. (國立交通大學光電所)
Ph.D.	2001.9~2004.6	Institute of Electro-Optical Engineering, National Chiao Tung University. (國立交通大學光電所)

- **Position at the institute**（職稱）**:**

Ph.D. of the Institute of Electro-Optical Engineering, National Chiao Tung University.
（國立交通大學光電所博士）

Publication List

I. Journal Papers

1. <u>**I-An Yao**</u>, Jin-Jei Wu and Shu-Hsia Chen: **"Three-dimensional simulation of the homeotropic to planar transition in cholesteric liquid crystals using the finite elements method"** *Jpn. J. Appl. Phys.* **43** 705 (2004).

2. <u>**I-An Yao**</u>, Jin-Jei Wu and Shu-Hsia Chen: **"Study of the transient phenomenon during homeotropic to planar transition in cholesteric liquid crystal cells"** *Jpn. J. Appl. Phys.* **43** 1488 (2004).

3. <u>**I-An Yao**</u>, Chien-Huang Liaw, Jin-Jei Wu and Shu-Hsia Chen: **"Direction-tunable cholesteric phase gratings"** *J. Appl. Phys.* (to be published).

4. <u>**I-An Yao**</u>, Jin-Jei Wu and Shu-Hsia Chen: **"Observation of electric-field-driven modulated textures in cholesteric liquid crystal cells"** *Jpn. J. Appl. Phys.* (accepted).

5. <u>**I-An Yao**</u>, Yin-chieh Lai, Jin-Jei Wu and Shu-Hsia Chen: **"Relaxation of a field-unwound cholesteric liquid crystal"** submitted to *Phys. Rev. E.*

II. International Conference Papers

1. Ting-Jui Chang, **I-An Yao**, Shu-Hsia Chen, Jung Y. Huang, and Jin-Jei Wu: **"Study on the electro-optical properties of weakly anchored twisted nematic liquid crystal cells"** *IDMC* p. 591 (2003).

2. **I-An Yao**, Jin-Jei Wu, Shu-Hsia Chen:**"Multidimensional simulation of the homeotropic to planar transition in cholesteric liquid crystals using the finite elements method"** *AM-LCD* p. 241 (2003).

3. **I-An Yao**, Jin-Jei Wu, Shu-Hsia Chen:**"Computer simulation of the similar-Helfrich deformation during the transient planar to planar transition in cholesteric liquid crystals"** *ASID* p. 616 (2004).

4. **I-An Yao**, Jin-Jei Wu, Shu-Hsia Chen:**"Computer simulation of the field-induced homogeneous to planar transition in cholesteric liquid crystals"** *ILCC* (2004).
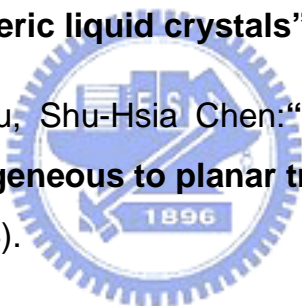
III. Local Conference Papers

1. Ting-Jui Chang, **I-An Yao**, Shu-Hsia Chen, Jung Y. Huang, and Jin-Jei Wu: **"Study on the electro-optical properties of non-rigidly anchored twisted nematic liquid crystal cells"** *OPT* p. 355 (2002).

2. **I-An Yao**, Jin-Jei Wu, and Shu-Hsia Chen:**"Effect of bias voltage on the homeotropic to planar relaxation in cholesteric liquid crystals"** *2003 中國液態晶體學會年會暨研討會論文集* p.52 (2003).

3. **I-An Yao**, Rui-Jie Xiang, Jin-Jei Wu, and Shu-Hsia Chen:**"Study on the field-induced homogeneous to planar relaxation in cholesteric liquid crystals"** *TDC* p.155 (2004).